

Earthquake networks based on similar activity patterns

Joel N. Tenenbaum,¹ Shlomo Havlin,² and H. Eugene Stanley¹

¹ *Center for Polymer Studies and Department of Physics,
Boston University, Boston, Massachusetts 02215, USA*

²*Minerva Center and Department of Physics,
Bar-Ilan University - Ramat-Gan 52900, Israel*

(Dated: January 21, 2013)

Abstract

Earthquakes are a complex spatiotemporal phenomenon, the underlying mechanism for which is still not fully understood despite decades of research and analysis. We propose and develop a network approach to earthquake events. In this network, a node represents a spatial location while a link between two nodes represents similar activity patterns in the two different locations. The strength of a link is proportional to the strength of the cross-correlation in activities of two nodes joined by the link. We apply our network approach to a Japanese earthquake catalog spanning the 14-year period 1985-1998. We find strong links representing large correlations between patterns in locations separated by more than 1000 km, corroborating prior observations that earthquake interactions have no characteristic length scale. We find network characteristics not attributable to chance alone, including a large number of network links, high node assortativity, and strong stability over time.

I. INTRODUCTION

Despite the underlying complexities of earthquake dynamics and their complex spatiotemporal behavior [1, 2], celebrated statistical scaling laws have emerged, describing the number of events of a given magnitude (Gutenberg-Richter law) [3], the decaying rate of aftershocks after a main event (Omori law) [4–6], the magnitude difference between the main shock and its largest aftershock (Bath law) [7], as well as the fractal spatial occurrence of events [8–11]. Recent work has shown that scaling recurrence times according to the above laws results in the distribution collapsing onto a single curve [12, 13]. However, while the fractal occurrence of earthquakes incorporates spatial dependence, it appears to embed isotropy in the form of radial symmetry, while the occurrence of real-world earthquakes is usually anisotropic [14].

To better characterize this anisotropic spatial dependence as it applies to such heterogeneous geography, network approaches have been recently applied to study earthquake catalogs [15–22]. These recent network approaches define links as being between successive events, events close in distance [19], or being between events which have a relatively small probability of both occurring based on three of the above statistical scaling laws [23]. These methods define links between singular events. In contrast, we define links between locations based on long-term similarity of earthquake activity. While earlier approaches capture the dynamic nature of an earthquake network, they do not incorporate the characteristic properties of each particular location along the fault. Various studies have shown [4, 24–27] that the interval times between earthquake events for localized areas within a catalog have distributions not well described by a Poisson distribution [28], even within aftershock sequences [27]. This demonstrates that each area not only has its own statistical characteristics [29], but also retains a memory of its events [24–26]. As a result, successive events may not be just the result of uncorrelated independent chance but instead might be dependent on the history particular to that location. If prediction is to be a goal of earthquake research, it makes sense to incorporate interactions due to long-term behavior inherent to a given location, rather than by treating each event independently. We include long-term behavior as such in this paper by considering a network of locations (nodes) and interactions between them (links), where each location is characterized by its long-term activity over several years.

II. DATA

For our analysis, we utilize data from the *Japan University Network Earthquake Catalog* (JUNEC), available online at <http://www.eic.eri.u-tokyo.ac.jp/CATALOG/junec/>. We choose the JUNEC catalog because Japan is among the most active and best observed seismic regions in the world. Because our technique is novel, this catalog provided the best avenue for employing our analysis. In the future, it may be possible to fine-tune our approach to more sparse catalogs.

The data in the JUNEC catalog span 14 years from 1 July 1985 - 31 December 1998 and are depicted in Fig. 1. Each entry in the catalog includes the date, time, magnitude, latitude, and longitude of the event. We found the catalog to obey the Gutenberg-Richter law [30] for events of magnitude 2.2 or larger. By convention, this is taken to mean that the catalog can be assumed to be complete in that magnitude range. However, because catalog completeness cannot be guaranteed for shorter time periods over a 14-year span, we also examine Gutenberg-Richter statistics for each non-overlapping two-year period (Fig. 2) [30]. We find that, though absolute activity varies by year, the relative occurrences of quakes of varying magnitudes does not change significantly for events between magnitude 2.2 and 5, where there is the greatest danger of events missing from the catalog.

Additionally, the data are spatially heterogeneous, as shown in Fig. 1. Most events take place either over land or off Japan's east coast. We remark to the reader that this is not an artifact of more detection equipment being located on land. The primary means for locating and detecting earthquake events involves using the S-waves and P-waves that emanate from the events. Seismic stations are capable of detecting these waves a great distance from their source. Both S-waves and P-waves [31] travel through the Earth's mantle, and the characteristic absorption distance, defined as the distance for wave amplitude to drop to $1/e$ of its original value, for body waves is on the order of 10,000 km [32]. Any event of magnitude 5.5 or larger, for example, is detectable anywhere on earth. Hence, the location of the detection equipment does not affect how accurately events are catalogued. Additionally, because the location of the Japanese archipelago is a consequence of seismic activity involving the Philippine and other tectonic plates, it is not surprising that most seismic events take place on or near the islands themselves.

III. METHOD

We partition the region associated with the JUNE catalog as follows: we take the northernmost, southernmost, easternmost, and westernmost extrema of all events in the catalog as the spatial bounds for our analysis. We partition this region into a 23×23 grid which is evenly spaced in geographic coordinates. Each grid square of approximate size $100 \text{ km} \times 100 \text{ km}$ is regarded as a possible node in our network. Results do not qualitatively differ when the fineness of the spatial grid is modified, in agreement with analogous work carried out by Ref. [20], using a different technique from ours [18]. However, 100 km boxes are a more physical choice, as 100 km is on the order of rupture length associated with earthquakes [33], which in turn is roughly equivalent to the aftershock zone distance for larger earthquakes [34].

For a given measurement at time t , an event of magnitude M occurs inside a given grid square. Similar to the method of Corral [27], we define the signal of a given grid square to form a time series $\{s_t\}$, where each series term s_t is related to the earthquake activity that takes place inside that grid square within the time window Δt , as described below.

Because events do not generally occur on a daily basis in a given grid square, it is necessary to bin the data to some level of coarseness. How coarse the data are treated involves a trade-off between precision and data richness.

We define the best results as those corresponding to the most prominent cross-correlations. To this end, we choose 90 days as the coarseness for our time series. This choice means that s_t will cover a time window of $\Delta t = 90$ days and s_{t+1} will cover the 90-day non-intersecting time period immediately following, giving approximately 4 increments per year. Additional analysis shows that results do not qualitatively differ by changing the time coarseness.

We refer to the time series $\{s_t\}$ belonging to each grid cell ij as that grid cell's signal. We define the signal that is related to the energy released in the the ij grid cell by

$$s_t(ij) \equiv \sum_{\ell=1}^{N_t(ij)} 10^{\frac{3}{2}M_t^\ell(ij)}, \quad (1)$$

where $N_t(ij)$ denotes the number of events that occur in t th time window in grid square ij . We choose this definition because the term $10^{\frac{3}{2}M}$ is proportional to the energy released from an earthquake of magnitude M [35]. The signal therefore is proportional to the total energy

released at a given location in a 90-day time period [36].

To define a link between two grid squares, we calculate the Pearson product-moment correlation coefficient $r_{x,y}$ between the two time series $\{x_t\}, \{y_t\}$ associated with those two grid squares [40]

$$r_{x,y} \equiv \frac{\langle XY \rangle - \langle X \rangle \langle Y \rangle}{\sigma_x \sigma_y}, \quad (2)$$

where $\langle \dots \rangle$ indicates the mean and σ_x, σ_y the standard deviations of the time series $\{x_t\}, \{y_t\}$.

We consider the two grid squares linked if $r_{x,y}$ is larger than a specified threshold value r_c , where r_c is a tunable parameter. As is standard in network-related analysis, we define the degree k of a node to be the number of links the node has. Note that our signal definition Eq. 1 involves an exponentiation of numbers of order 1. This means that the energy released, and therefore the cross-correlation between two signals, is dominated by large events. Examples of signals with high correlation are shown in Fig. 3.

To confirm the statistical significance of $r_{x,y}$, we compare $r_{x,y}$ of any two given signals with $r_{x,y}$ calculated by shuffling one of the signals. We also compare $r_{x,y}$ with the cross-correlation $\tilde{r}_{x,y}(\tau)$ we obtain by time-shifting one of the signals by varying time increments τ ,

$$\tilde{r}_{x,y}(\tau) \equiv r(s_{x,t}, s_{y,t+\tau}), \quad (3)$$

where τ is in units of 90 days. Further, we impose periodic boundaries

$$t + \tau \equiv (t + \tau) \mod t_{max}, \quad (4)$$

where t_{max} is the length of the series. Our justification for these boundaries is that events in the distant past (>10 years) should have nominal effects on the present, while they also provide typical background noise for comparison.

We note that over 14-year time period 1985-1998, the overall observed activity increases in the areas covered by the catalog. To ensure that the $r_{x,y}$ values we calculate are not simply the result of trends in the data, we compare our results to those obtained with linearly detrended data [37]. We find that the trends do not have a significant effect. For example, using $r_c = 0.7$, we obtain 815 links, while detrending the data results in only 3 links dropping below the threshold correlation value. For $r_c = 0.6$, we obtain 1003 links,

while detrending results in only 3 links dropped. Additionally, after detrending, 94% of correlation values stay within 2% of their values.

IV. RESULTS

As described above, we compare $\tilde{r}_{x,y}(0) \equiv r_{x,y}$ of Eq. 3 between signals at different locations at the same point in time with $\tilde{r}_{x,y}(\tau)$ and with correlation coefficient obtained by shuffling one of the series. Shuffling or time-shifting by a single time step (representing 90 days) reduces $\tilde{r}_{x,y}$ to within the margin of significance, as shown in Fig. 4. Shuffling the signal also reduces We find a large number of links with cross-correlations far larger than their shuffled counterparts. The number of links exceeds that of time-shuffled data by roughly 3σ - 8σ , depending on choice of r_c as shown in Fig. 5 (a). However, as shown, there are still many links that can be regarded as the result of noise. We therefore further examine the difference between the number of links found in time-shuffled data and the number found in the original data (Fig. 5 (b)). We find that the fraction of “real” links in general increases with r_c .

A significant fraction of these links connect nodes farther apart than 1000 km, as can be seen in Fig. 6. This is consistent with the finding that there is no characteristic cut-off length for interactions between events [20, 23], corroborated by Fig. 7, showing the number of links a network has at a given distance as a fraction of the number of links that are possible from choosing any two nodes in the potential network. Distances shorter than 100 km have sparse statistics due to the coarseness of the grid while distances greater than 2300 km have sparse statistics due to the finite spatial extent of the catalog. Within this range, the fraction of links observed drops off approximately no faster than a power law. We find qualitatively similar results when we adjust the grid coarseness.

Our results, shown in Fig. 6, are anisotropic, with the majority of links occurring at approximately 37.5 degrees east of north. This is roughly along the principal axis of Honshu, Japan’s main island, and parallel to the highly active fault zone formed by the subduction of the Philippine and Pacific tectonic plates under the Amurian and Okhotsk plates respectively. High degree nodes (i.e. nodes with a large number of links) tend to be found in the northeast and northcentral regions of the JUNEK catalog and are notably not strongly associated with the locations in the catalog that are most active, which we discuss in further

detail below.

In network physics, we often characterize networks by the preference for high-degree nodes to connect to other high-degree nodes. The strength of this preference is quantified by the network's assortativity, defined as

$$A \equiv r_{k_1, k_2}, \quad (5)$$

where r is the Pearson correlation coefficient given by Eq. (2). The series k_1 and k_2 are found as follows: iterating through all entries i, j in the adjacency matrix [38], the degree of each node i is appended to the series $\{k_1\}$ and the degree of the node j that i is linked to is appended to the series $\{k_2\}$. The assortativity coefficient thus gives a correlation of node degree within the network. If each node of degree k connects only to nodes of the same degree, the two series $\{k_1\}$ and $\{k_2\}$ will be identical and $A=1$. Networks like the network of paper coauthorship have positive assortativity, while those of the World-Wide Web and of many ecological and biological systems have negative assortativity [39].

Fig. 8 shows that the networks resulting from our procedure are highly assortative with assortativity generally increasing with r_c . The finding of positive correlation between the degree of a node and the degree of its neighbors is consistent with an analogous finding [20] with Iranian data, using a different technique from ours [18]. For comparison we show the assortativity obtained by using time shuffled networks. Since assortativity of the original networks is far higher than those of shuffled systems, the high assortativity cannot be due to a finite size effect or to the spatial clustering displayed in the data, since time shuffling preserves location. We investigate the nature of the high-degree nodes and find that high degree is not a matter of more events being nearby, as there is a slight tendency for higher degree nodes to actually have *longer* distance links on average than low degree nodes. Additionally, we found that node degree is essentially independent of both maximum earthquake size and number of events.

Because Fig. 5 shows, as mentioned above, that many links can be regarded as the result of noise, we investigate the stability of links over time (Fig. 9). Similarity of the network between the first seven years (1985-1992) and the second seven years (1992-1998) in the catalog is found as follows. We find the set of links that satisfy $r \geq r_c$ in both the 1985-1992 network and the 1992-1998 network, and create a series out of the respective link strengths (correlations) in the 1985-1992 network. We create another series using the same

links, now using the corresponding strengths from the 1992-1998 network. We then correlate the two series using the Pearson correlation coefficient given by Eq. (2). We find that the network is far more stable over time than counterpart results given by shuffling the time series (Fig. 9). Because one would expect large correlations that arise purely from noise to have no “memory” from one time period to another, the finding of network stability over several years is consistent with our result that these links are not simply the result of chance.

V. DISCUSSION AND CONCLUSIONS

To summarize our results, we have introduced a novel method for analyzing earthquake activity through the use of networks [41]. The resulting networks (i) display links with no characteristic length scale, (ii) display far more links than expected from chance alone, (iii) are far more assortative, and (iv) display significantly more link stability over time. The lack of a characteristic length scale is consistent with previous work and underscores the difficulty in making accurate predictions. The statistically significant nature of all of these results is consistent with the possibility of the presence of hidden information in a catalog, not captured by existing models or previous earthquake network approaches.

We thank K. Yamasaki for useful discussions, and the DTRA, ONR, European EPI-WORK and LINC projects, and the Israel Science Foundation for financial support.

-
- [1] Y. Y. Kagan and D. D. Jackson, *J. Geophys. Res.* **96**, 419 (1991).
 - [2] D. Marsan, C. J. Bean, S. Steacy, and J. McCloskey, *J. Geophys. Res.* **105**, 28081 (2000).
 - [3] B. Gutenberg and C.F. Richter, *Bull. Seismol. Soc. Am.* **34**, 185 (1944).
 - [4] F. Omori, *J. Coll. Sci. Imp. Univ. Tokyo* **7**, 111 (1894); see the recent work of M. Bottiglieri, L. de Arcangelis, C. Godano, and E. Lippiello, *Phys. Rev. Lett.* **104**, 158501 (2010).
 - [5] T. Utsu, *Geophys. Magazine* **30**, 521 (1961).
 - [6] T. Utsu, Y. Ogata, R. S. Matsu’ura. *J. of Phys. of the Earth* **43**, 1 (1995).
 - [7] M. Bath, *Tectonophysics*, **2**, 483 (1965).
 - [8] Y. Y. Kagan and L. Knopoff, *Geophys. J. R. Astron. Soc.* **62**, 303 (1980).
 - [9] D. Turcotte, *Fractals and Chaos in Geology and Geophysics* (Cambridge University Press,

- Cambridge, 1997).
- [10] P. G. Okubo and K. J. Aki, J. Geophys. Res. **92**, 345 (1987).
 - [11] T. Hirata, Pure and Applied Geophysics, **131**, 157 (1989).
 - [12] P. Bak, K. Christensen, L. Danon, and T. Scanlon, Phys. Rev. Lett. **88**, 178501 (2002).
 - [13] A. Corral, Phys. Rev. E **68**, 035102(R) (2003).
 - [14] R. Olsson, Geodynamics **27**, 547 (1999).
 - [15] S. Abe and N. Suzuki, J. Geophys. Res. **108**, 2113 (2003).
 - [16] S. Abe and N. Suzuki, Physica A **332**, 533 (2004).
 - [17] S. Abe and N. Suzuki, Physica A **350**, 588 (2005).
 - [18] S. Abe and N. Suzuki, Eur. Phys. J. B **59**, 9397 (2007).
 - [19] J. Davidsen, P. Grassberger, and M. Paczuski, Geophys. Res. Lett. **33**, L11304 (2006); Phys. Rev. E **77**, 066104 (2008).
 - [20] N. Lotfi and A. H. Darooneha, Eur. Phys. J. B **85**, 23 (2012).
 - [21] D. Pastén, S. Abe, V. Muñoz, and N. Suzuki, arXiv:1005.5548v1 (2010).
 - [22] S. Abe, D. Pastén, and N. Suzuki, Physica A **390**, 1343 (2011).
 - [23] M. Baiesi and M. Paczuski, Phys. Rev. E **69**, 066106 (2004).
 - [24] V. N. Livina, S. Havlin, and A. Bunde, Phys. Rev. Lett. **95**, 208501 (2005).
 - [25] E. Lippiello, L. de Arcangelis, and C. Godano, Phys. Rev. Lett. **100**, 038501 (2008).
 - [26] S. Lennartz, V. N. Livina, A. Bunde, and S. Havlin, Europhys. Lett. **81**, 69001 (2008).
 - [27] A. Corral, Phys. Rev. Lett. **92**, 108501 (2004).
 - [28] D. Sornette and L. Knopoff, Bull. Seismol. Soc. Am. **87**, 789 (1997).
 - [29] J. Davidsen and C. Goltz, Geophys. Res. Lett. **31**, L21612 (2004).
 - [30] The Gutenberg-Richter law states that the number of events N in the catalog greater than a certain magnitude M has an exponential dependence, i.e. $\log N = a - bM$, where a and b are empirically observed constants with b typically ≈ 0 .
 - [31] P-waves and S-waves are the body waves which originate at an earthquake and travel through the earth. They are the primary means for locating an event. See: K. E. Bullen and B. A. Bolt, *An Introduction to the Theory of Seismology* (Cambridge University Press, Cambridge, 1993).
 - [32] W. Lowrie, *Fundamentals of Geophysics* p.98 (Cambridge University Press, Cambridge, 2007).
 - [33] D. L. Wells and K. H. Coppersmith, Bull. Seismol. Soc. Am. **84**, 974 (1994).

- [34] K. I. Konstantinou, G. A. Papadopoulos, A. Fokaefs, K. Orphanogiannaki, *Tectonophysics* **403**, 95 (2005).
- [35] K. Arora, A. Cazenave, E. R. Engdahl, R. Kind, A. Manglik, S. Roy, K. Sain, S. Uyeda, and H. K. Gupta, *Encyclopedia of Solid Earth Geophysics, Volume 1*, p.213 (Springer, 2011).
- [36] We note that this term is similar in appearance though distinct from the cumulative Benioff strain [42], the predictive power of which is hotly contested in geophysics [43, 44]. However, our technique does not use this term to make predictive statements about any individual events in a specific location, but rather allows us to observe patterns in the similarity of behavior across different locations.
- [37] To detrend the data, we obtain a best fit linear trend for each time series and subtract it from the series. We calculate the cross-correlation between the detrended sequences.
- [38] The adjacency matrix a_{ij} fully specifies a given network. $a_{ij} = 1$ denotes a link between node i and node j while $a_{ij} = 0$ denotes no link.
- [39] M. E. J. Newman, *Phys. Rev. Lett.* **89**, 208701 (2002).
- [40] W. Feller, *An Introduction to Probability Theory and Its Applications*, San Diego, 1997, edited by J. B. Kadtko, A. Bulsara (AIP, Woodbury, 1997).
- [41] For comparison, we also carried out our analysis with another three signal definitions that we omit here:
 - (1) “average magnitude”: $s_t^{(1)}(ij) \equiv N_{ij}^{-1} \sum_{\ell=1}^{N_{ij}} M_t^\ell(ij)$, where $M_t^\ell(ij)$ is the magnitude of the event and $N_t(ij)$ is the total number of events occurring in the 90-day time window t in the grid square ij .
 - (2) “number of events”: $s_t^{(2)}(ij) \equiv N_t(ij)$, with the symbols as defined in (a).
 - (3) “magnitude sum”: $s_t^{(3)}(ij) \equiv \sum_{\ell=1}^{N_t(ij)} M_t^\ell(ij)$.

All three of these alternative definitions fail to give results significantly better than the shuffled data that are robust with respect to the various adjustable parameters.
- [42] D. D. Bowman, G. Ouillon, C. G. Sammis, A. Sornette, and D. Sornette, *J. Geo-phys. Res.* **103**, 24,359 (1998).
- [43] K. R. Felzer, T. W. Becker, R. E. Abercrombie, G Ekstrom, J. R. Rice, *J. Geophys. Res.* **107**, 2190 (2002).
- [44] J. L. Hardebeck, K. Felzer, and A. J. Michael, *J. Geophys. Res.* **113**, B08310 (2008).

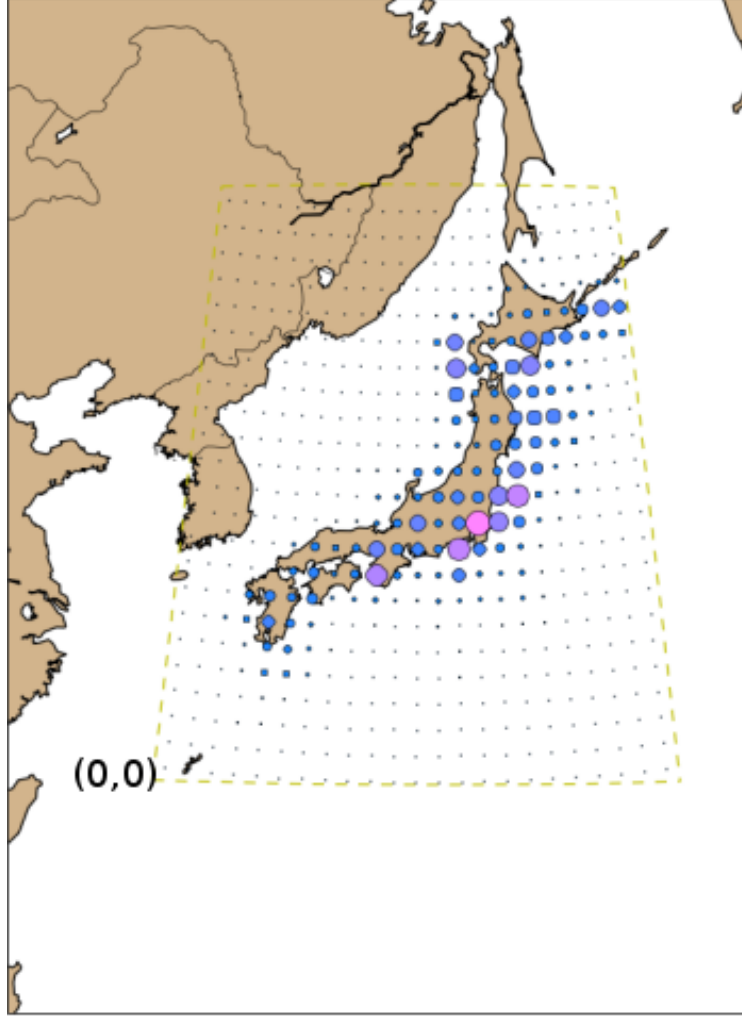


FIG. 1: (Color online) Number of events by location in the JUNE catalog, shown in a 23×23 mesh. Larger circles with brighter colors denote more events. The JUNE catalog clusters spatially, with most activity occurring on the eastern side of Honshu, Japan's main island.

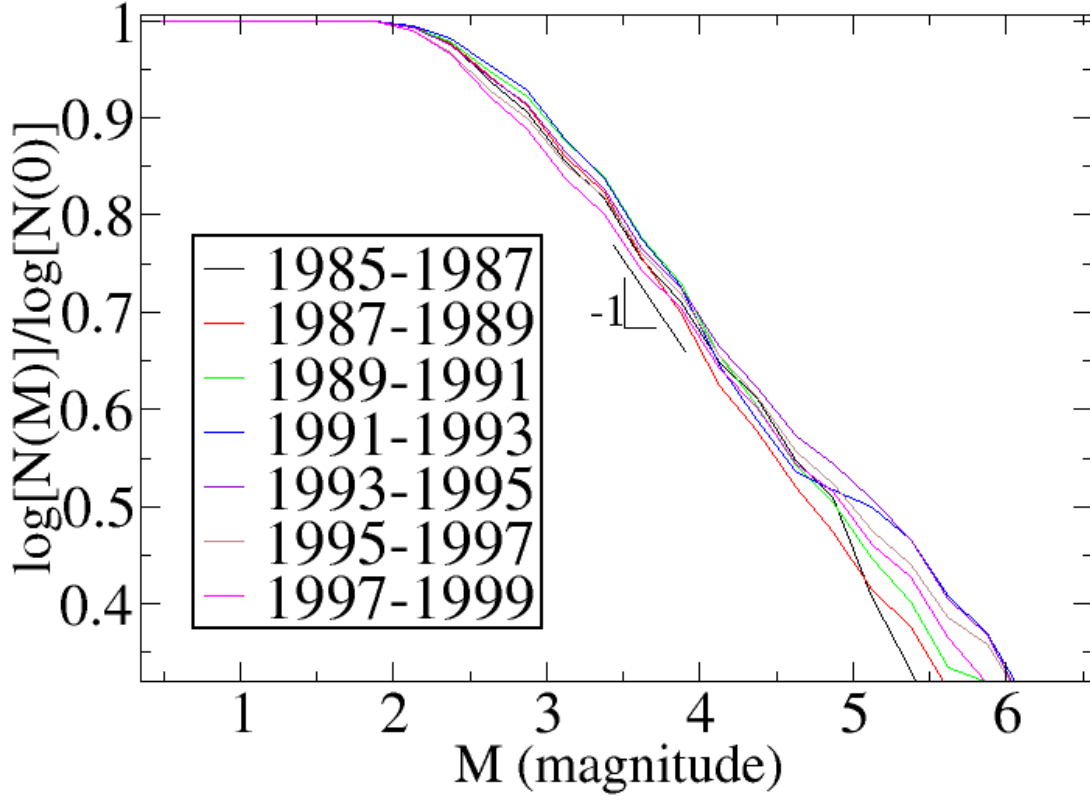


FIG. 2: (Color online) Demonstrating that the magnitude above which the Gutenberg-Richter law is obeyed is approximately constant from year to year. To this end, we provide Gutenberg-Richter statistics for the JUNE C catalog over separated 2-year periods. The Gutenberg-Richter law states that the number N of events greater than a given magnitude M obeys $\log N = a - bM$, with $b \approx 1$.

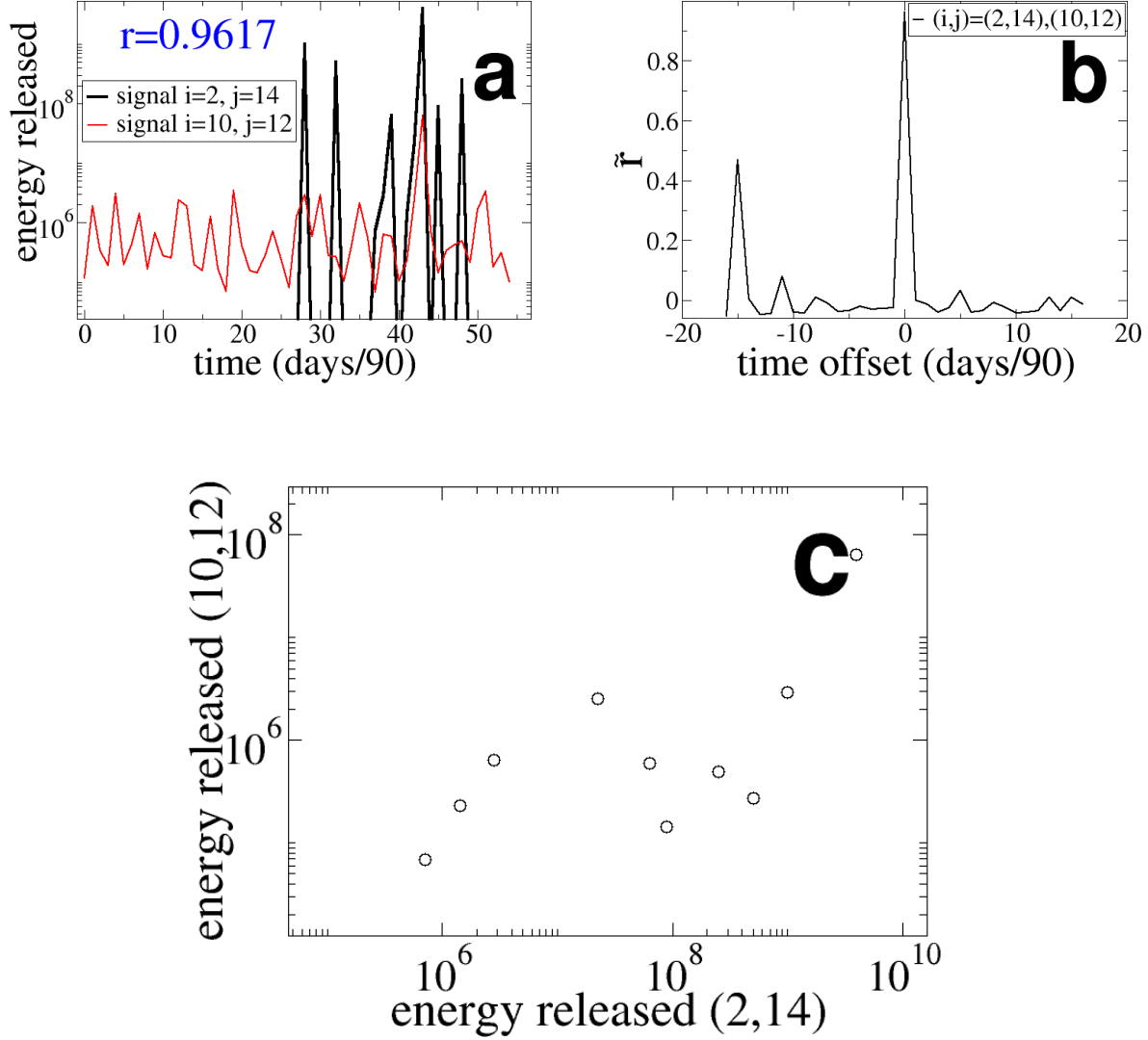


FIG. 3: (Color online) Examples of highly correlated signals, as defined in Eq. (1), with values of (i, j) marked above: (a) Two signals with Pearson correlation coefficient $r = 0.9617$, associated with locations 878 km apart, (b) the corresponding \tilde{r} as a function of time offset as defined by Eq. 3. (c) Corresponding scatterplot of (a) with signal $(i, j) = (10, 12)$ plotted against signal $(i, j) = (2, 14)$. Each point corresponds to a single point in time for the simultaneous signals of $(10, 12)$ and $(2, 14)$. Note that because the signal is defined in terms of exponentiation that large events dominate the correlation, just as large events dominate the total energy released in an earthquake catalog.

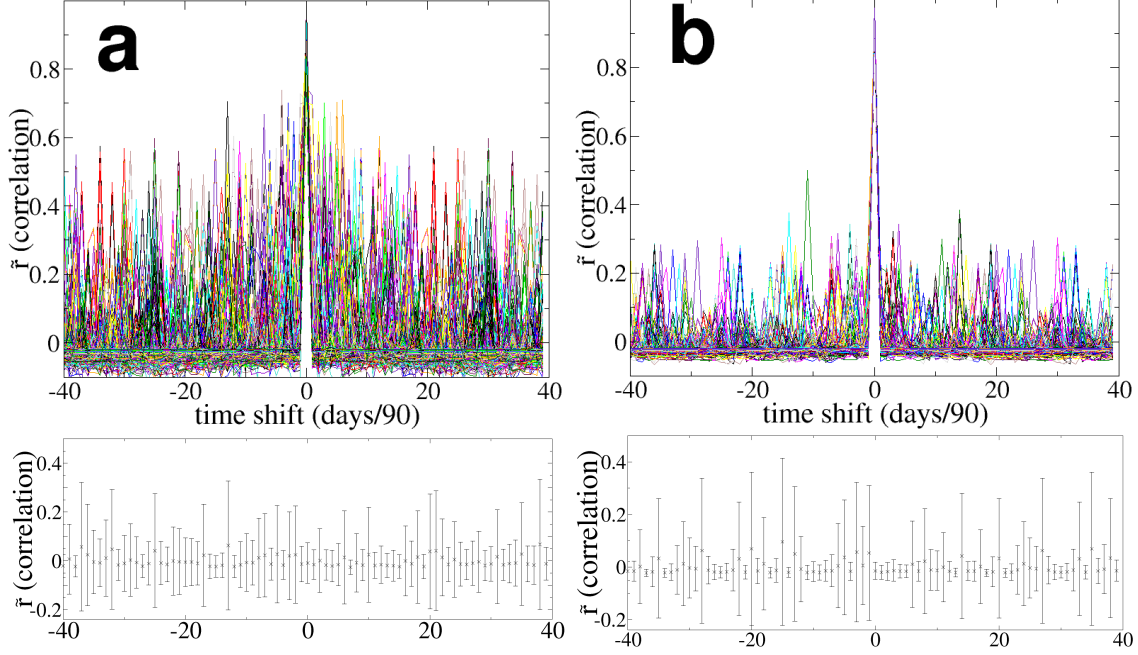


FIG. 4: (Color online) Testing the statistical significance of cross-correlations to demonstrate that correlations observed are stronger than ambient noise. For each pair of signals with a cross-correlation $r \geq r_c$, we shift one of the signals in time and calculate the new correlation coefficient. Each colored line is a comparison of a pair of signals, as described by Eq. 3. Note the strong peak at $t = 0$ corresponding to signals being compared at the same time. Offsetting the signals in time results in lower cross-correlation, dropping to the level of noise in the actual data. As a control, we shuffle the signals and calculate the cross-correlation for different time shifts (shown below each figure). Cross-correlation between various pairs of signals vs. time offset. Shown are links for which (a) $\tilde{r}(0) \geq r_c = 0.7$ and (b) $\tilde{r}(0) \geq r_c = 0.9$.

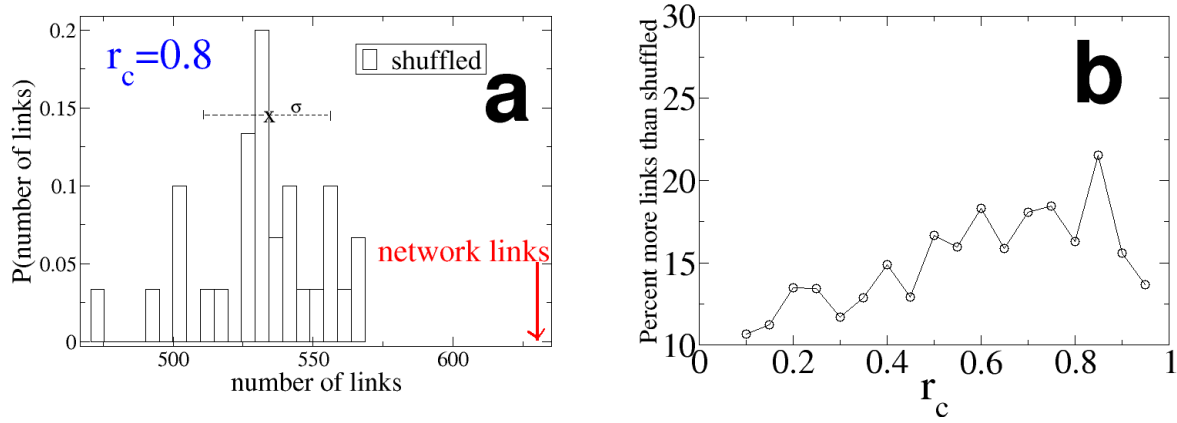


FIG. 5: (Color online) Demonstration that empirical data show far more links than time shuffled data. (a) In black is the distribution of the number of links obtained in the network after time shuffling the data many times. A link corresponds to a correlation coefficient between two signals of $r \geq r_c$. Shown is the case $r_c = 0.8$. Actual results, shown in red (color online), are greater than 5σ from the mean of the shuffled distribution, about 17% more links than the mean of the shuffled distribution. (b) Results are similar for other values of r_c . We note that the fraction of links we can regard “real” or meaningful in general increases with r_c .

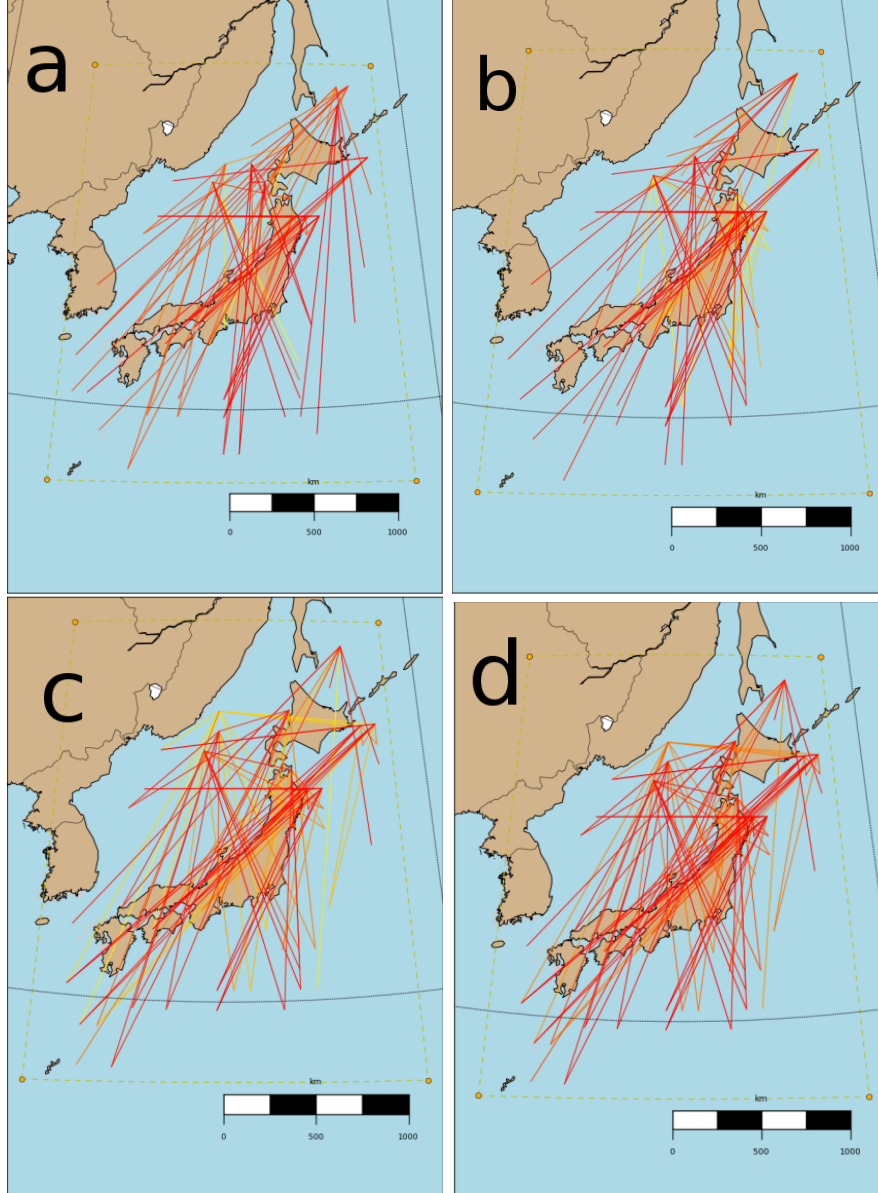


FIG. 6: (Color online) Network links superimposed on a map of the Japanese archipelago, including Japan's main island Honshu. Note that links are anisotropic and primarily lie parallel to the principal axis of Honshu. Shown are links satisfying $r \geq r_c$ that are connected to high-degree nodes ($k > k_{min}$). Darker colors (red online) indicate stronger links (i.e. stronger cross-correlations). Links shown satisfy (a) $r_c = 0.9$, $k_{min} = 5$, (b) $r_c = 0.8$, $k_{min} = 7$, (c) $r_c = 0.7$, $k_{min} = 8$, (d) $r_c = 0.5$, $k_{min} = 8$. These choices for r_c and k_{min} give approximately 70, 70, 90, and 90 links respectively.

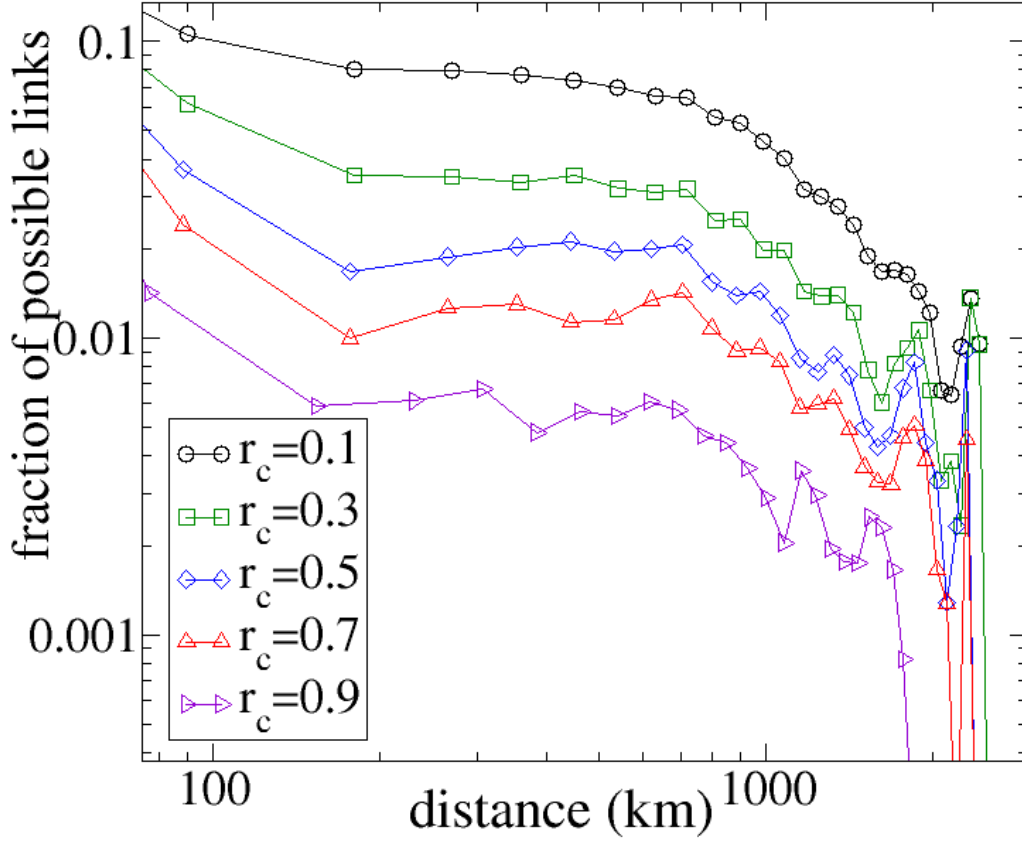


FIG. 7: (Color online) Demonstration that links have no characteristic length scale. To this end, we show the number of network links at a given distance as a fraction of how many links are possible at that distance from choosing any pairs of nodes. Distances less than 100 km have sparse statistics due to the coarseness of the spatial grid, while distances greater than 2300 km have sparse statistics due to the finite spatial extent of the catalog.

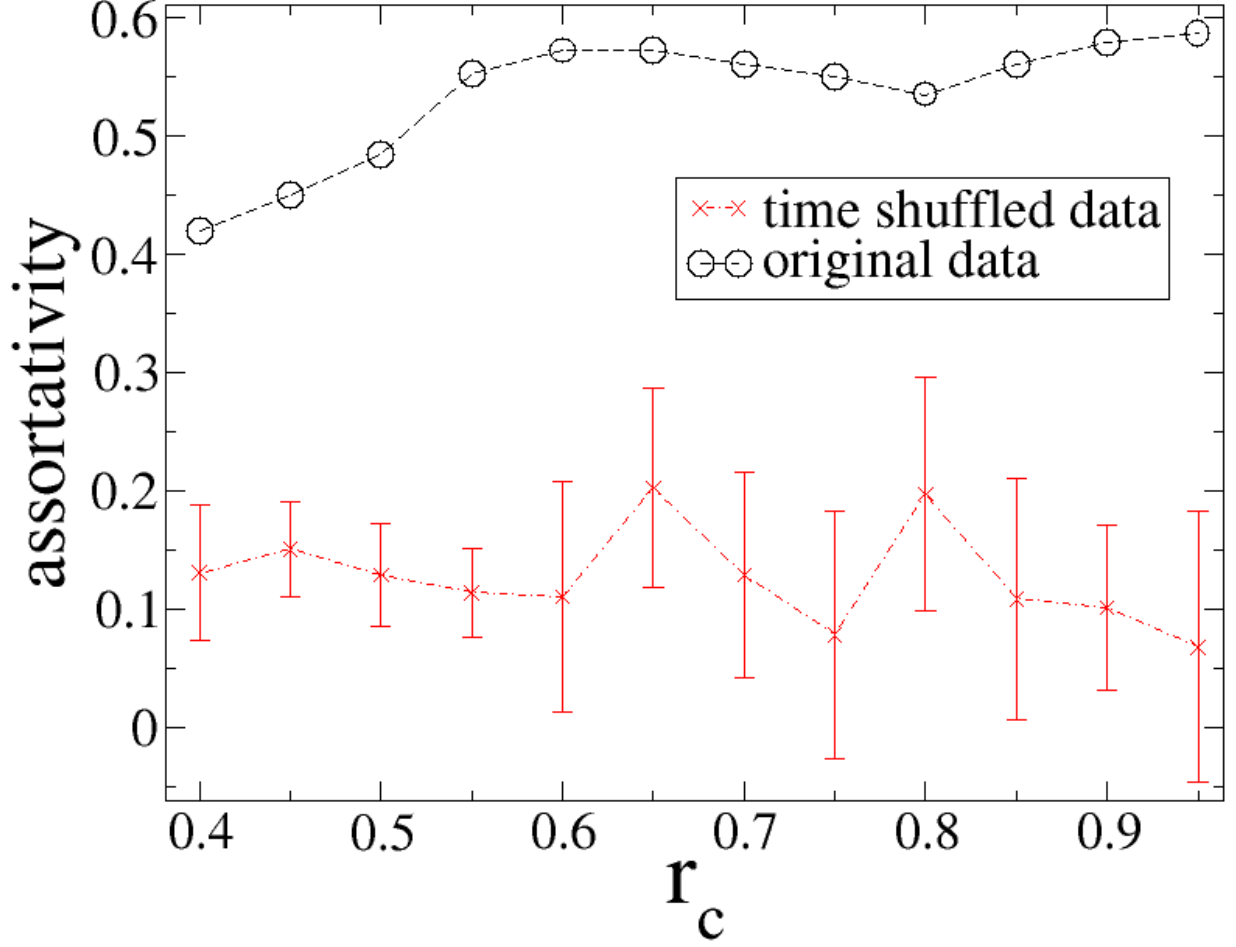


FIG. 8: (Color online) Demonstration that earthquake networks are highly assortative (see Eq. (5)) for a wide range of r_c , with assortativity A generally increasing with r_c . $A > 0$ indicates that high-degree nodes tend to link to high-degree nodes and low-degree nodes tend to link to low-degree nodes. For comparison assortativity values obtained from networks using time-shuffled data demonstrate that these findings are neither a finite-size effect nor a result of spatial clustering, since time-shuffling preserves location.

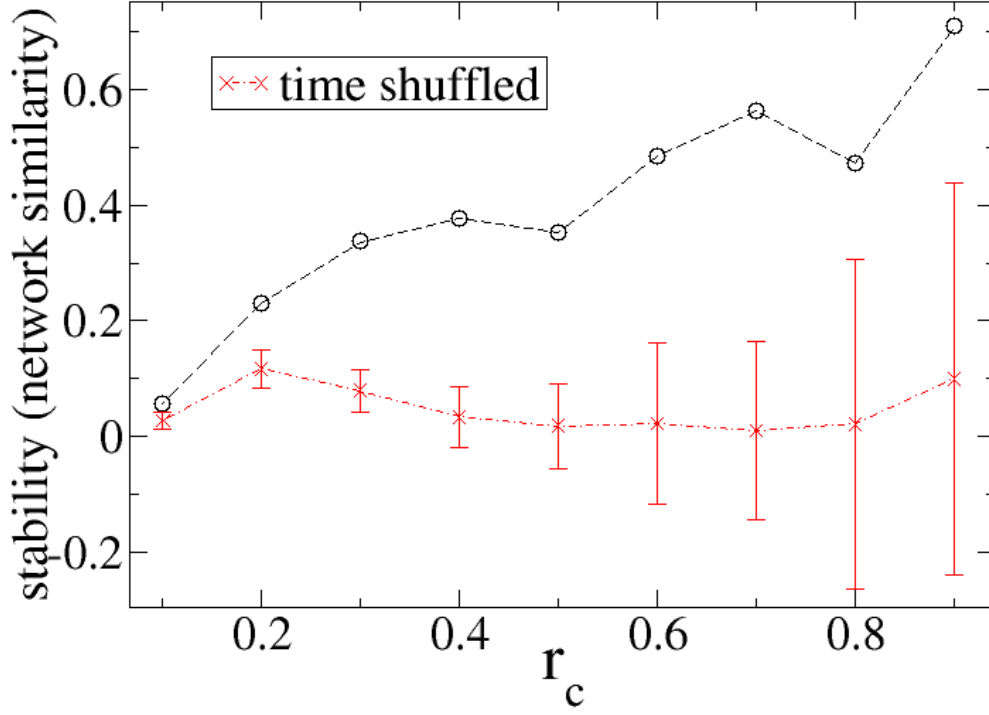


FIG. 9: (Color online) Correlation networks display stability over time. Shown is the similarity of the 1985-1992 network with the 1992-1998 network. Similarity is obtained by (i) selecting the set of links that satisfy $r \geq r_c$ in both networks, (ii) making one series out of the strengths (cross-correlation) in the 1985-1992 network and creating another series out of the corresponding strengths in the 1992-1998 network and (iii) correlating the two series using the Pearson cross-correlation coefficient given by Eq. (2).